Geochimica et Cosmochimica Acta, Vol. 69, No. 22, pp. 5307–5316, 2005

0016-7037/05 $30.00 + .00

doi:10.1016/j.gca.2005.06.023

Mechanisms of uranium mineralization by the yeast *Saccharomyces cerevisiae*

Toshihiko Ohnuki,[1,*] Takuo Ozaki,[1] Takahiro Yoshida,[1] Fuminori Sakamoto,[1] Naofumi Kozai,[2] Eiichi Wakai,[3] Arokiasamy J. Francis,[4] and Haruyuki Iefuji[5]

[1]Advanced Science Research Center, Japan Atomic Energy Research Institute, Shirakata-2, Tokai, Ibaraki 319-1195, Japan
[2]Department of Environmental Sciences, Japan Atomic Energy Research Institute, Shirakata-2, Tokai, Ibaraki 319-1195, Japan
[3]Department of Material Science, Japan Atomic Energy Research Institute, Shirakata-2, Tokai, Ibaraki 319-1195, Japan
[4]Environmental Sciences Department, Brookhaven National Laboratory, Upton, New York 11973, USA
[5]Environmental Research Division, National Research Institute of Brewing, 3-7-1 Kagamiyama, Higashi-Hiroshima, Hiroshima 739-0046, Japan

(*Received September* 1, 2004; *accepted in revised form June* 27, 2005)

Abstract—We determined the association of uranium in yeast cells *S. cerevisiae* grown in medium containing high (1 g · L^{-1}) or low (0.2 g · L^{-1}) concentrations of phosphate after exposure for 96 h to a 4×10^{-4} mol · L^{-1} U(VI) solution at pH 3.2 or 4.7. The analysis was made using a field emission scanning electron microscope equipped with energy dispersive spectroscopy (FESEM-EDS), transmission electron microscopy (TEM), and visible diffuse reflectance spectrometry. Cells grown in the high-phosphate medium rapidly accumulated U(VI) from solution at pH 3.2 over the first 24 h, followed by a slow uptake until 96 h, whereas in cells grown in low-phosphate medium, U(VI) accumulation reached a steady state within 24 h. FESEM-EDS analyses revealed the formation of a U(VI)-bearing precipitate on the yeast cells grown in high-phosphate medium after only 48 h exposure; no precipitate was detected on cells grown in low-phosphate medium up to 96 h. These results suggest that sorption onto the cell surfaces was the dominant process initially. Analysis of the U(VI)-bearing precipitates by all three methods demonstrated the presence of H-autunite, $HUO_2PO_4 \cdot 4H_2O$. Thermodynamic calculations suggest that the chemical compositions of the solutions containing yeast grown in high-phosphate medium were undersaturated with respect to H-autunite, but were supersaturated with ten times more U(VI) and P than were actually observed. Apparently, the sorbed U(VI) on the cell surfaces reacts with P released from the yeast to form H-autunite by local saturation. The U(VI) uptake by yeast cells grown in high phosphate medium at pH 4.7, along with the thermodynamic calculation, indicated that more H-autunite is precipitated in neutral pH solution than in acid solution. Thus, U(VI)-phosphate mineralization on the cells of microorganisms should be taken into account for predicting U(VI) mobility in the environment. *Copyright © 2005 Elsevier Ltd*

1. INTRODUCTION

Over the last two decades, the interactions of uranyl ion with microorganisms have been extensively studied because of the potential for using these organisms to remediate contaminated waste streams and groundwater (Strandberg et al., 1981; Macaskie and Dean, 1985; Lovley et al., 1991; Lovley et al., 1993; Suzuki and Banfield, 1999; Haas et al., 2001). Iron-reducing, fermentative, and sulfate-reducing bacteria are known to reduce uranium(VI) to uraninite (UO_2; Lovley et al., 1991; Francis et al., 1994). Uraninite has low solubility and is very stable in reducing environments. However, it readily dissolves upon exposure to oxidizing water to form uranyl aqueous complexes (Langmuir, 1978). The mobility of these complexes is affected by their adsorption on organic and inorganic substances and by the formation of secondary uranyl minerals (e.g., Bruno et al., 1995; Murakami et al., 1997; Duff et al., 2002).

Many investigators have reported the formation of U(VI) minerals by microorganisms, for example, the formation of H-autunite ($HUO_2PO_4 \cdot 4H_2O$) around the cells of *Citrobacter* sp. (Macaskie et al., 1992; Young and Macaskie, 1995; Jeong et al., 1997) and of *Bacillus sphaericus* (Knopp, et al., 2003); others observed the accumulation of U(VI) as needlelike fibrils on the cell surface of *S. cerevisiae* (Strandberg, et al., 1981; Volesky and May-Philips, 1995). However, the mechanisms whereby microorganisms cause the precipitation of uranium are poorly understood, and the U-bearing precipitates have not been properly characterized.

We investigated the uptake of U(VI) by *S. cerevisiae* and characterized the U(VI) minerals formed on the surface of cells by three methods: field emission scanning microscopy (FESEM) and energy dispersive spectroscopy (EDS), transmission electron microscopy (TEM), and visible diffuse reflectance spectrometry. We choose to study *S. cerevisiae* because its cell is larger than of prokaryotes, and hence, is readily amenable for characterization by microprobe and spectroscopic techniques. We also undertook thermodynamic calculations to determine U(VI) mineralization.

2. MATERIALS AND METHODS

2.1. Uranium Uptake Experiments

S. cerevisiae X-2180 was grown in 100 mL of bacto yeast nitrogen base (YNB) medium (ammonium sulfate, 5 g · L^{-1}; L-histidine mono-hydrochloride, 10 mg · L^{-1}; LD-methionine, 20 mg · L^{-1}; LD-tryptophan, 20 mg · L^{-1}; biotin, 2 μg · L^{-1}; calcium pantothenate, 400 μg · L^{-1}; folic acid, 2 μg · L^{-1}; inositol, 2000 μg · L^{-1}; niacin, 400 μg · L^{-1}; *p*-aminobenzoic acid, 200 μg · L^{-1}; pyridoxine hydrochloride, 400 μg · L^{-1}; riboflavin, 200 μg · L^{-1}; thiamine hydrochloride, 400 μg · L^{-1}; boric acid, 500 μg · L^{-1}; copper sulfate, 40 μg · L^{-1}; potassium iodide, 100 μg · L^{-1}; ferric chloride, 200 μg · L^{-1}; manganese sulfate, 400 μg · L^{-1}; sodium molybdate, 200

* Author to whom correspondence should be addressed (ohnuki@sparclt.tokai.jaeri.go.jp).

$\mu g \cdot L^{-1}$; zinc sulfate, 400 $\mu g \cdot L^{-1}$; magnesium sulfate, 0.5 $g \cdot L^{-1}$; sodium chloride, 0. 1 $g \cdot L^{-1}$; and calcium chloride, 0. 1 $g \cdot L^{-1}$) containing 1 $g \cdot L^{-1}$ or 0.2 $g \cdot L^{-1}$ phosphorus in a 500 mL flask. The cells were incubated on a shaker at 110 rpm for 24 to 36 h at 30°C. The cells at the stationary growth phase were harvested by centrifugation at 3000 rpm for 20 min; they were washed three times with 0.1 $mol \cdot L^{-1}$ NaCl solution. Yeasts grown in medium containing 1.0 $g \cdot L^{-1}$ or 0.2 $g \cdot L^{-1}$ phosphorus are termed yeast P1.0 and yeast P0.2, respectively. Twenty mg (dry weight) of yeast P1.0 or P0.2 cells were transferred into polycarbonate tubes to which 20 mL of 4×10^{-4} $mol \cdot L^{-1}$ U(VI) in 0.01 $mol \cdot L^{-1}$ NaCl solution was added. The pHs of the samples were adjusted to 3.2 and 4.7 for yeast P1.0, and to 3.2 for yeast P0.2 with 1 $mol \cdot L^{-1}$NaOH and 1 $mol \cdot L^{-1}$ HCl solution. Duplicate samples were incubated for 96 h at 25°C. No U(VI) was precipitated in a yeast-free 4×10^{-4} $mol \cdot L^{-1}$ U(VI) solution at pHs between 3 and 5 for 96 h, indicating that U(VI) was undersaturated compared to U(VI)-oxy/hydroxides. Further, U(VI) sorption on the tube's walls was less than 0.1% of the initial concentration over 96 h. Samples were withdrawn at intervals of 2, 6, 24, 48, and 96 h for yeast P1.0, and at 24, 48, and 96 h for yeast P0.2, and then centrifuged at 3000 rpm for 20 min to separate the cells and supernatant. The pH and U(VI) concentration in the supernatant was determined.

2.2. Analytical Methods

Uranium(VI) was measured in a liquid scintillation counter (Packard Tri-Carb 2550TR/AB) using liquid scintillation cocktails (Packard Ultima-Gold AB and F). Phosphorus was assessed by inductively coupled plasma atomic-emission spectrometry (ICP-AES; Seiko SPS 7700). The concentrations of P in 0.01 M NaCl solutions of pH 3.2 containing no U(VI), but the same amount of the yeast P1.0 as in the U(VI) accumulation experiments, also were measured at 24, 48, and 96 h.

The U(VI) accumulated in yeast P1.0, yeast P0.2, and control yeast cells not exposed to U(VI) was analyzed by field emission scanning electron microscopy (FESEM; JEOL-6330F) at an operating voltage of 20 kV. Elemental analysis of the accumulated U(VI) in yeast cells was carried out by FESEM equipped with an energy dispersive X-ray analyzer (EDS; JED-2140) at an operating voltage of 20 or 25 kV.

Spectra of dark field images were obtained with visible diffuse reflectance spectrometry for U(VI) accumulated yeast. The analytical spot size was 20 μm. Spectra of the U(VI)-oxide mineral schoepite, $UO_3 \cdot 2H_2O$, and U(VI)-phosphate mineral autunite, $Ca(UO_2)_2(PO_4)_2 \cdot 10H_2O$, served as reference standards. The instrument consists of a microscope (BH-2, Olympus) and visible spectrometer units, having a grating grid and CCD (charge-coupled device) camera; details of the instrument and analysis are described elsewhere (Nagano et al., 2002). We used the Kubelka-Munk equation to transform these spectra into absorbance spectra (Kubelka and Munk, 1931).

Yeast cells that had exposed to U(VI) at pH 3.2 were fixed and analyzed as thin sections by transmission electron microscopy TEM (Hitachi HF-2000) operating at 200 kV in the following way: After the cells remaining in the suspensions were washed with deionized water, they were prefixed with agar, and then fixed for 1 h in cacodylic acid buffer solution containing 2% paraformaldehyde and 1.25% glutaraldehyde at pH 7.4, dehydrated through an ethanol, and processed into Spurr resin (TAAB). Thin sections were cut at 100 nm with an ultramicrotome (RMC MT-7000 Ultra), and mounted on Formvar- and carbon-coated 200-mesh copper grids.

Elemental analysis was carried out by EDS attached to the TEM using a Kevex Sigma system software package. Selected area electron diffraction (SAED) was applied for analyzing the crystal form of U mineral.

2.3. Viability of Yeast Exposed to U(VI) Solution

The viability of the yeast cells was estimated by the classical spread-plating method. A 0.1 mL U(VI) solution (two replicates) containing yeast P1.0 at pH 3.2 was sampled at 24, 48, 72, and 96 h after exposure. The solutions were diluted with sterilized deionized water to the appropriate dilution and plated on the YPD (1.0% yeast, 2.0% pepton, 2.0% dextrose) agar media. Colonies were counted 3 to 4 days after incubation at 30°C. The P1.0 cells exposed to U(VI) solution for 96 h at pH 3.2 were inoculated on a 0.2 μm membrane filter mounted on the YPD agar medium for 12 h at 30°C. After washing with deionized water and drying, the cells were observed under FESEM-EDS. In the viability experiments, all solutions were sterilized by filtration through a 0.2 μm membrane filter.

Table 1. Calculated values of log(Q/K) for H-autunite with final pHs and concentrations of U, and P*.

Sample #	Condition pH	Condition Time	Concentration ($mol \cdot L^{-1}$) P	Concentration ($mol \cdot L^{-1}$) U	Log Q/K
1	3.2	24	1×10^{-6}	7.0×10^{-5}	−3.1
2	3.2	48	3.2×10^{-6}	2.0×10^{-5}	−3.2
3	3.3	96	7.3×10^{-6}	1.2×10^{-5}	−3.0
4	4.7	24	DL[b]	8.0×10^{-5}	NC[c]
5	4.7	48	6.3×10^{-6}	2.5×10^{-5}	0.6
6	4.9	96	1.5×10^{-5}	1.3×10^{-5}	0.8
7	3.2	96	1.4×10^{-6}	8.0×10^{-5}	−2.9
2A[a]	3.2	48	3.2×10^{-5}	2.0×10^{-4}	0.73

* The calculations were carried out using measured final pHs and concentrations of U and P in the U(VI) solutions after contact with the yeast P1.0 (Samples 1 to 6) samples for 24, 48, and 96 h and P0.2 (Sample 7) sample for 96 h.

[a] Samples 2A is for calculating where the P and U(VI) concentrations were changed to 3.2×10^{-5} and 2.0×10^{-4} $mol \cdot L^{-1}$, respectively, with the condition that the other input data for the respective calculations were the same as those for Sample 2.

[b] DL represents below the detection limit, 6.5×10^{-6} $mol \cdot L^{-1}$.

[c] NC denotes not calculated.

2.4. Thermodynamic Calculation of U(VI) Minerals

We calculated the thermodynamic stabilities of U(VI) minerals such as H-autunite, $HUO_2 \cdot PO_4 \cdot 4H_2O$, using the EQ3NR software package (Wolery, 1992). Because H-autunite was definitively identified in the analyses of U(VI)-bearing precipitates (see below), we excluded the U(VI) minerals of oxyhydroxides, silicates, arsenates, and carbonates from the calculation. The dissolution of H-autunite is expressed by the following equation:

$$HUO_2PO_4 = UO_2^{2+} + HPO_4^{2-} \quad (1)$$

The possibility of other U(VI) minerals being present was examined using thermodynamic data from Grenthe et al. (1992) for H-autunite (log K = −12.6686 at 25°C) and from chemical thermodynamic data of the U(VI)-phosphoric acid system. Similar data were taken from Wolery (1992) for dissolved and mineral species other than the U-phosphoric species. The thermodynamic database for uranyl phosphate solids and soluble species may be incomplete. For instance, we excluded data for $UO_2(HPO_4)_2^{2-}$ (Langmuir, 1978), following Grenthe et al. (1992) and Bennett and Read (1992).

Using the EQ3NR computer code, we calculated log Q/K for H-autunite, where Q was the activity product of the species in a reaction, using U(VI) and P concentrations, and pH in the U(VI) solutions at 24, 48, and 96 h after contact with yeast P 1.0 at pHs 3.2 and 4.7 (Table 1). For comparison, we calculated log Q/K for H-autunite using pH, U(VI), and P concentrations in the U(VI) solution at 96 h after the exposure to yeast P0.2. In this calculation carbonate is assumed to be in equilibrium with the atmospheric condition.

3. RESULTS

3.1. Time-Dependent Accumulation of U(VI) by *S. cerevisiae*

Figure 1 plots the time-dependent average accumulated fractions for yeast P1.0 at pHs 3.2 and 4.7, and for yeast P0.2 at pH 3.2. The accumulation by yeast P1.0 at both pHs increased rapidly with exposure time up to 24 h, followed by a gradual

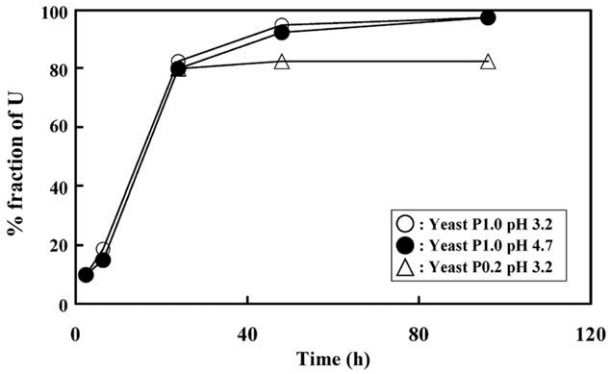

Fig. 1. Time-dependent accumulated fractions of U(VI) on yeast P1.0 at pH 3.2, yeast P1.0 at pH 4.7, and yeast P0.2 at pH 3.2.

increase until 96 h. Equilibrium was not attained within 96 h. The value for the accumulation by yeast P0.2 at 24 h was similar to that for yeast P1.0 at pH 3.2, but thereafter remained constant between 24 and 96 h. The pH did not change up to 48 h. At 96 h, the pH increased from 3.2 to 3.3 for yeast P1.0, but for yeast P0.2 it remained unchanged; for samples incubated at pH 4.7, it increased to 4.9.

Concentrations of P released into solution from yeast P 1.0 at pH 3.2 rose with increasing exposure time to U(VI) (Fig. 2). After 24 h, the levels were higher than those at pH 4.7. However, at both 48 and 96 h after exposure, this trend was reversed, and the concentration of P at pH 4.7 was higher than that at pH 3.2. The level of P in solution for yeast P0.2 at 96 h was lower than those from yeast P1.0 at both pH 3.2 and 4.7. The release of P from yeast P1.0 in the U(VI) free solution at pH 3.2 increased with time, and was higher than that from cells exposed to U(VI) solution.

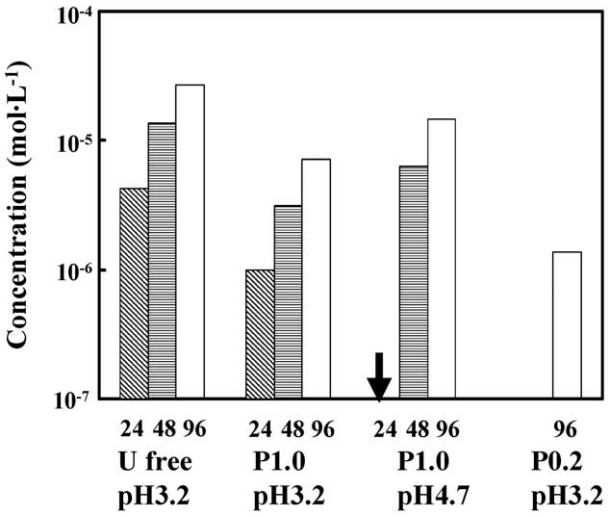

Fig. 2. P concentrations released from yeast P1.0 at pH 3.2, yeast P1.0 at pH 4.7, and yeast P0.2 at pH 3.2 into the U(VI) solution, and from yeast P1.0 into the U-free solution. The arrow shows that P concentration is below the detection limit.

3.2. Analysis by FESEM-EDS

Figures 3 and 4 show the FESEM images of yeast without U treatment (controls) and the U(VI) accumulated yeasts P1.0 and P0.2 at 2, 24, 48, and 96 h after exposure to uranium. Figure 5 depicts the energy dispersive spectroscopy spectra of these same groups. No U(VI)-bearing precipitate (Fig. 3a) and no U peak in the EDS spectrum were observed in unexposed yeast cells (Fig. 5, spectrum 1).

For yeast P1.0 exposed for 2 h to U(VI) in a solution at pH 3.2, no U(VI)-bearing precipitate was visible in the FESEM image (Fig. 3b). However, the corresponding U M_α peak intensity in the EDS spectrum of these cells (measured in the region shown by black arrow in Fig. 3b) was ~0.3-fold that of the P K_α peak (Fig. 5, spectrum 2). At 6 and 24 h after this exposure, similar FESEM images were obtained of the U(VI) accumulated precipitate as at 2 h, but the peak intensity of the U M_α peaks had risen to 0.5-fold that of the P K_α peaks. These results indicate that no U(VI)-bearing precipitate was present up to 24 h after exposure, even though uranium accumulated on the yeast.

The FESEM image of the yeast P1.0 at pH 3.2 at 48 h after U(VI) exposure (Fig. 3c) revealed distinct bright precipitates on the cells, as denoted by the white arrow A; only one bright area (Fig. 3c) was detected in a region of ~50 × 50 μm^2. The intensity of the U M_α peak in the EDS spectrum of intact cells (arrow A) was half of the P K_α peak (data not shown). An enlarged FESEM image of the yeast cells with bright precipitates (Fig. 3d) disclosed that the needlelike fibril precipitates, ~1 to 2 μm long, had directly developed from the yeast cells. The intensity of the U M_α and the P K_α peaks appearing in the EDS spectrum of the region B in Figure 3d (Fig. 5, spectrum 3) then were equivalent. The FESEM images from different regions of the section (Fig. 3e,f) showed that the needlelike fibril U(VI)-bearing precipitates developed from ruptured cells (arrow C in Fig. 3e), whereas the ~500-nm-long precipitates (arrow D in Fig. 3f) developed directly from the cell.

The FESEM image of the U(VI) accumulated cells of yeast P 1.0 at pH 3.2 at 96 h after exposure (Fig. 4a) exhibited both bright and dark regions; the former occurred every several μm. An enlarged image of the bright region (Fig. 4b) revealed needlelike fibril precipitates, ~1 to 2 μm long, (white arrow A) on the yeast cells. According to the EDS spectrum of this region (Fig. 5, spectrum 4), these precipitates contained U and P, and the intensity of the U M_α peak was comparable to that of the P K_α peak. By comparison, the intensity ratio of these peaks in the EDS spectra of the gray regions in Figure 4a (Fig. 5, spectrum 5) was ~0.5.

Similar FESEM images and EDS spectra to those of yeast P1.0 at pH 3.2 were obtained at 2, 6, and 24 h after exposing this yeast to a uranium solution at pH 4.7. Here, the FESEM image at 48 h after U(VI) exposure (Fig. 3g) displayed ~500-nm-long U(VI)-bearing precipitates (arrow E) occurring directly on the cells. After 96h, the image (Fig. 4c) exhibited bright and dark regions. The intensity ratios of the U M_α to P K_α peak in the EDS spectra of the gray regions in Figure 4c (Fig. 5, spectrum 6) was ~0.5. Further, granular precipitates of ~0.7 μm in length were apparent in the enlarged image from the bright region (Fig. 4d). The corresponding EDS spectrum of region B (Fig. 5, spectrum 7) indicated that these granular

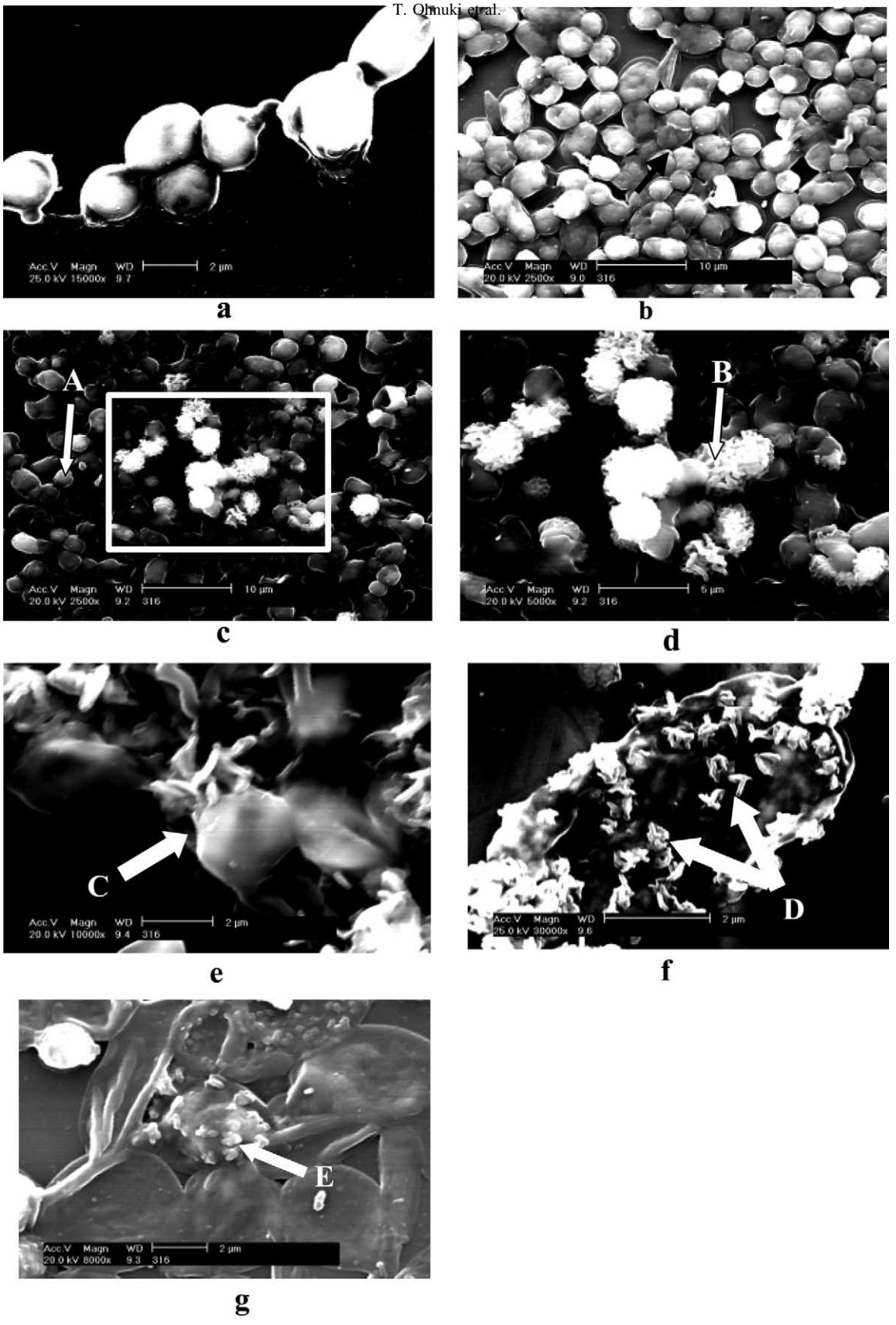

Fig. 3. (a) Field emission scanning electron micrograph images of control yeast; (b) the U(VI) accumulated yeast P1.0 at pH 3.2 at 2 h after the U(VI) exposure; (c) the U(VI) accumulated yeast P1.0 at 48 h after the U(VI) exposure at pH 3.2; (d) the enlarged image of the region shown by rectangle in c; (e, f) the U(VI) accumulated yeast P1.0 at 48 h after the U(VI) exposure at pH 3.2 (different positions from c); and (g) the U(VI) accumulated yeast P1.0 at 48 h after the U(VI) exposure at pH 4.7. Symbols A and B, E with arrows and black arrow in (b) indicate position analyzed by EDS. Symbol C with arrow shows ruptured yeast, and symbols D and E show U(VI)-bearing precipitates. See text for details.

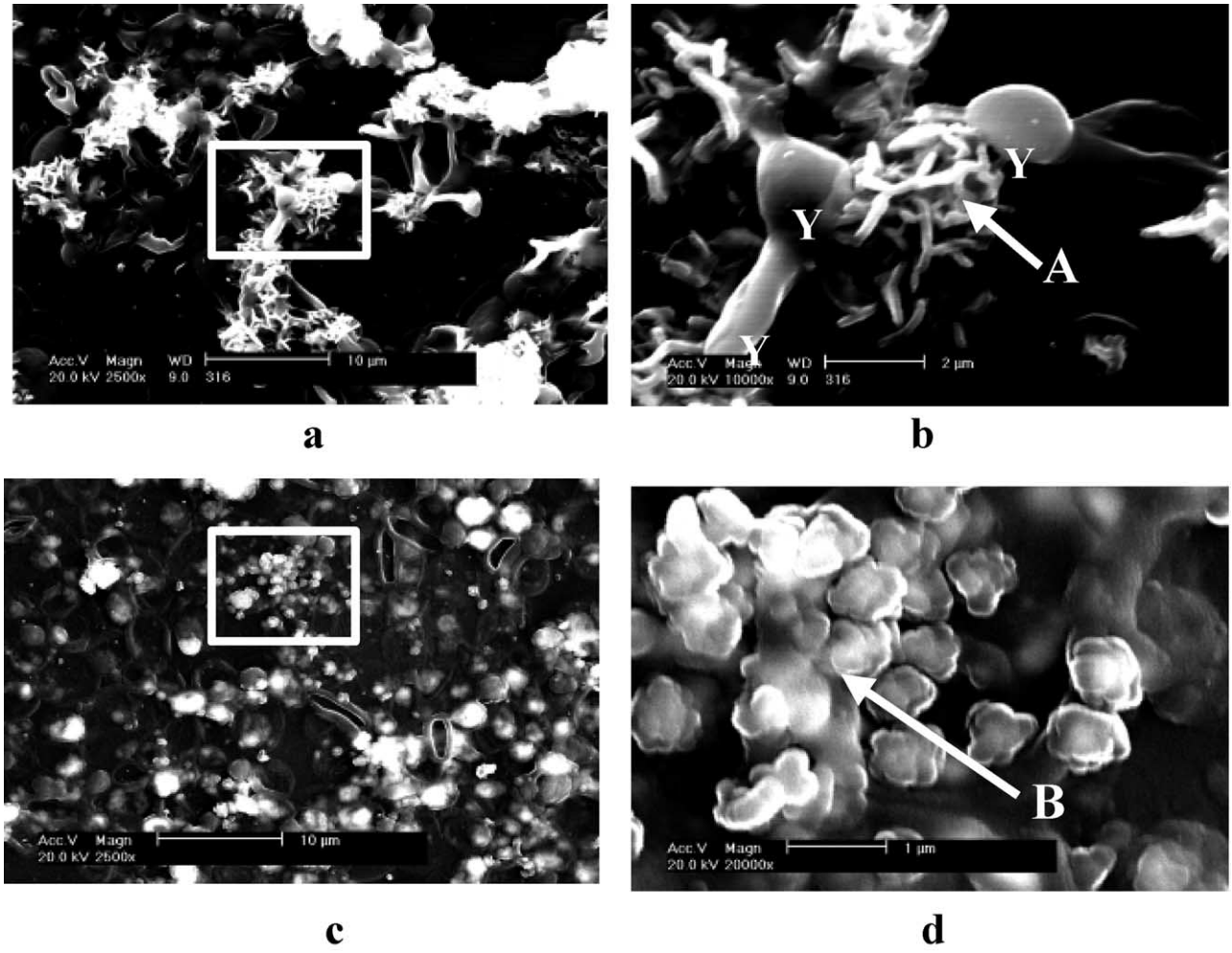

Fig. 4. Field emission scanning electron micrograph (FESEM) images of the U(VI) accumulated cells of yeast P1.0 at 96 h after the exposure to U(VI) solutions at pH 3.2 (a and b) and 4.7 (c and d). Images in (b) and (d) are the enlarged regions denoted by rectangles in (a) and (c), respectively. Symbols of A and B with arrows indicate the positions analyzed by EDS. The symbol Y indicates the yeast cell.

precipitates contained U and P, and the intensity of the U M_α peak was comparable to that of the P K_α peak.

These results suggest that the U(VI)-bearing precipitates were generated after exposure to the U(VI) solution, and that their morphology at pHs 3.2 and 4.7 differed. No U(VI) precipitates were apparent on/around the cells in FESEM images of yeast P0.2 after U(VI) exposure for 96 h (image not shown). The intensity of the U M_α peak in the corresponding EDS spectrum (not shown) was ~0.5-fold that of the P K_α peak. These findings confirmed that U(VI)-bearing precipitates did not form on the cells of yeast P0.2, even though they accumulated uranium.

3.3. Visible Diffuse Reflectance Spectrometry and TEM Analyses

The visible absorbance spectra of the U(VI) accumulated cells of yeast P1.0 at 96 h after exposure to the U(VI) solution at pH 3.2 (Fig. 6) showed four absorption peaks between 400 and 440 nm; the peaks also were observed at pH 4.7 after 96 h.

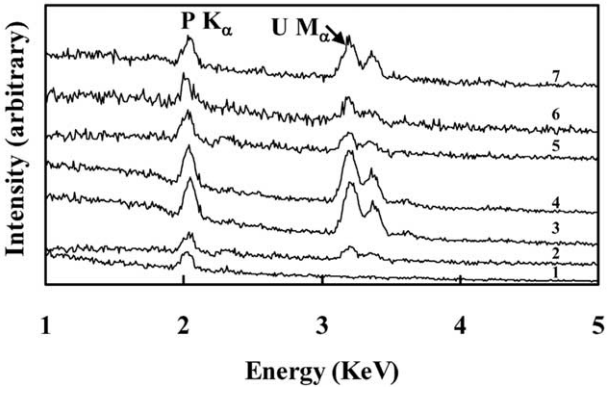

Fig. 5. Energy dispersive spectrometry spectra of control yeast (1), region in Figure 3b (2), bright region B in Figure 3d (3), bright region shown by arrow A in Figure 4b (4), dark region in Figure 4a (5), dark region in Figure 4c (6) and bright region shown by arrow B in Figure 4 d (7).

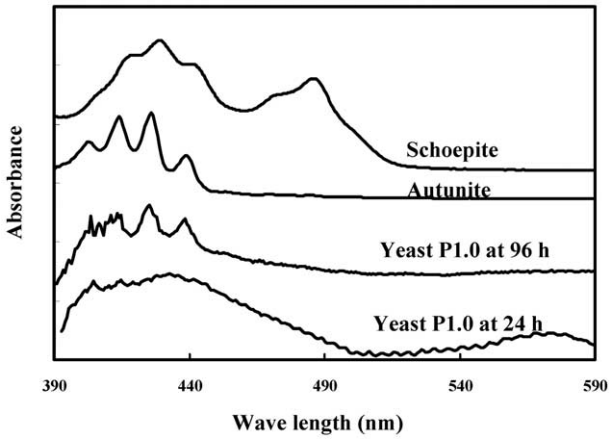

Fig. 6. Visible absorbance spectra of yeast P1.0 at pH 3.2 at 24 and 96 h after the U(VI) exposure. The visible absorbance spectra of schoepite and autunite are shown as reference standards.

The spectrum of the U(VI) accumulated cells of yeast P1.0 (Fig. 6) at 96 h differed from that of schoepite, but resembled that of the uranyl phosphate mineral (autunite), wherein four absorption peaks also were identified. This signifies that the precipitates on the cells of yeast P1.0 at pHs 3.2 and 4.7 at 96 h were not amorphous ones, but were uranyl phosphate crystalline minerals.

The four absorption peaks between 400 and 440 nm did not appear in the visible absorbance spectrum of the U(VI) accumulated cells of yeast P 1.0 at 24 h after immersion in the U(VI) solution at pH 3.2 (Fig. 6), nor in the spectra collected from the U(VI) accumulated cells of yeast P1.0 at pH 3.2 at 2 and 6 h, and yeast P1.0 at pH 4.7 at 2, 6, and 24 h after the exposure. Seemingly, U(VI) phosphate mineral was not formed within 24 h after exposure. Interestingly, no absorption peaks of U(VI) phosphate minerals were identified in the visible absorbance spectra of the U(VI) accumulated cells of yeast P1.0 at pHs 3.2 and 4.7 at 48 h after exposure and the U(VI) accumulated cells of yeast P0.2 at pH 3.2 at 24, 48, and 96 h after the exposure (data not shown).

Cells of different densities were observed in the TEM images of thin sections of the U(VI) accumulated yeast cells (Fig. 7a). One kind of cell was not covered by dense material (arrow heads in Fig. 7a), but in the second kind of cell, prominent dense needlelike fibrils apparently had grown out from the cells' surfaces (framed by a rectangle). A close-up image of a

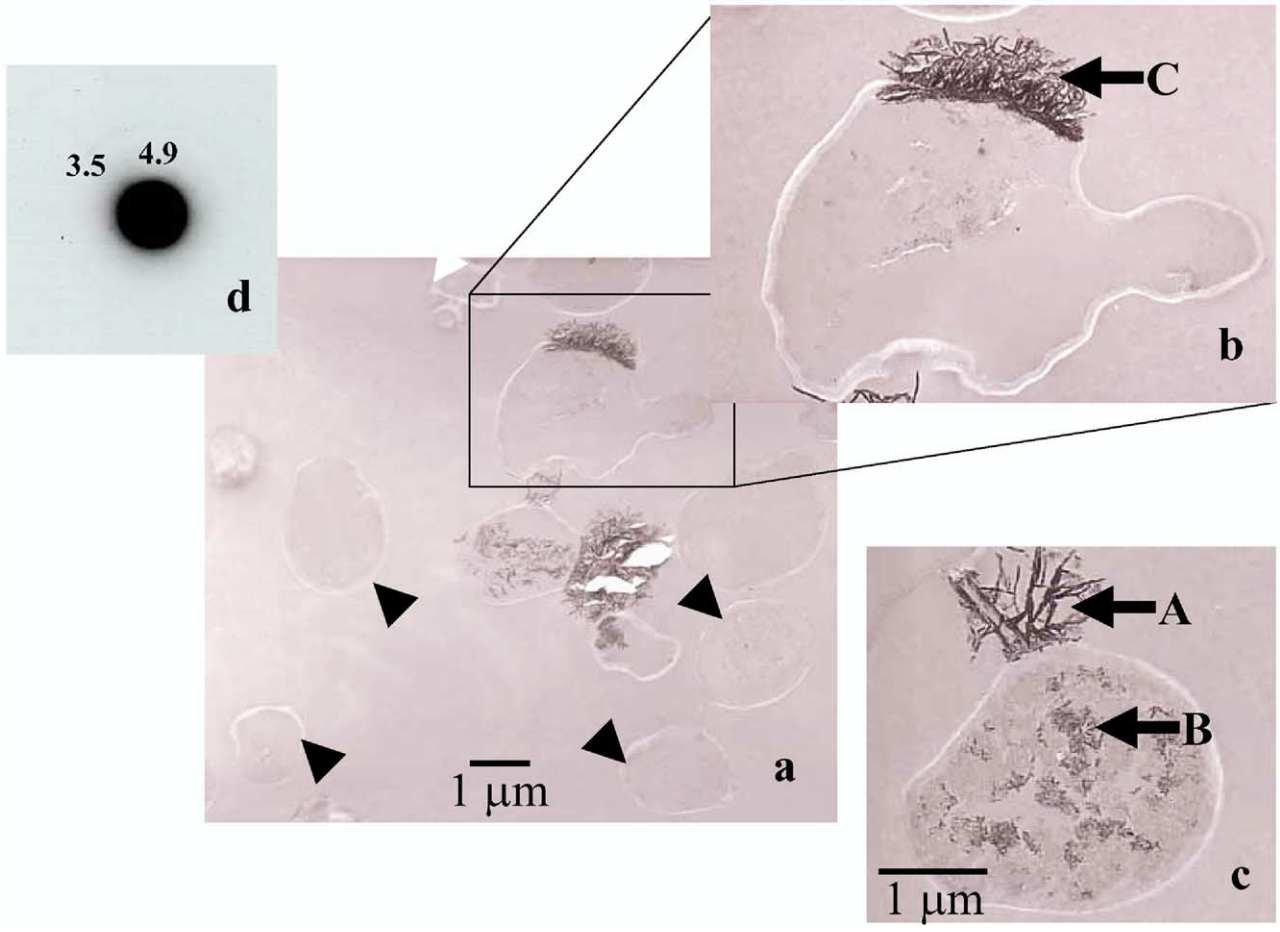

Fig. 7. (a) TEM image of thin section of the U(VI) accumulated yeast P1.0. (b) Enlarged image of the U(VI) accumulated cells in (a). (c) TEM image of the cell accumulating U(VI) outside (arrow A) and inside (arrow B). (d) Selected area electron diffraction pattern of dense region of yeast indicated by arrow C in (b).

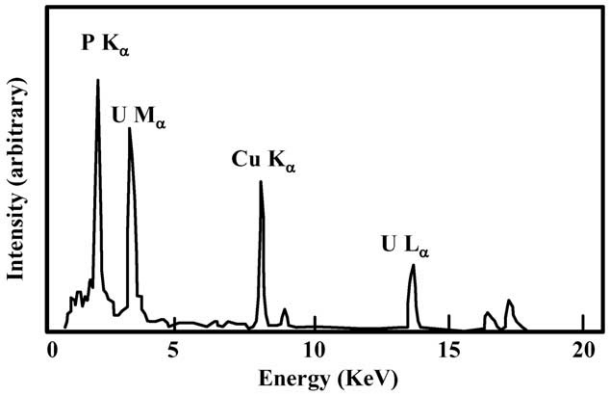

Fig. 8. EDS spectrum of the U(VI) precipitates shown by arrow C in Figure 7b. Cu originates from the Cu grid.

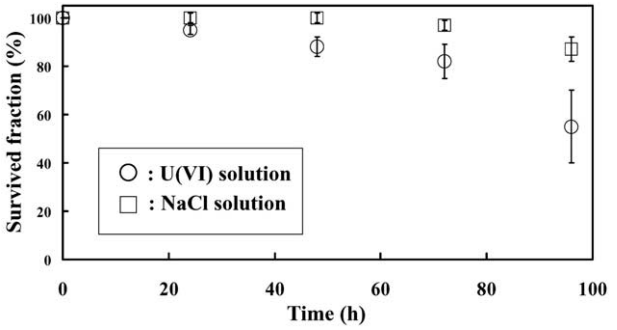

Fig. 9. The viability of yeast during U(VI) accumulation. The viability was estimated by the spread-plate technique as described in the text. U(VI) solution and NaCl solution indicate yeast exposed to a 4×10^{-4} mol · L^{-1} U(VI) solution and a 0.01 mol · L^{-1} NaCl solution, respectively. Each point represents the mean of two independent experiments in duplicate. The bar designates one standard deviation.

cell with dense material (Fig. 7b) demonstrated that the precipitates did not cover the entire cell surface, but emerged at its ruptured regions. The TEM image of cells at different positions (Fig. 7c) from that in Figure 7a showed precipitates both outside (arrow A) and inside (arrow B) the cell. The SAED pattern (Fig. 7d) of the needlelike fibrils (arrow C in inset a in Fig. 7) revealed diffraction spots corresponding to 4.9 and 3.5 Å. Their EDS analysis (arrow C in inset a in Fig. 7) showed that they contained U and P (Fig. 8).

3.4. Thermodynamic Calculation of H-Autunite

Table 1 gives the values of log Q/K calculated for H-autunite. For yeast P1.0 at pH 3.2, the log Q/K was negative at 24, 48, and 96 h after exposure to U(VI) solution, suggesting that chemically the solution was undersaturated with respect to H-autunite. Thus, H-autunite was not formed merely by precipitation in the U(VI) solution up to 96 h after exposure. However, if we assume that the P or U(VI) concentration was 10 times higher than actual concentrations, the values of log Q/K would be positive at 48 h. Therefore, if the concentration of P or U(VI) is higher at the cell surface than in the bulk solution, H-autunite can be precipitated by local saturation.

At pH 4.7, the log Q/K was ~0 at 48 and 96 h after exposure. Accordingly, the actual solutions may be supersaturated at these times. The log Q/K was not calculated at 24 h because P levels were below the detection limit (6.5×10^{-7} mol · L^{-1}).

3.5. Viability

The viability of yeast cells was not drastically affected by lengthening exposure to the 4×10^{-4} mol · L^{-1} U(VI) solution (Fig. 9). More than 80% of yeast cells were viable after 48 h, and ~60% were alive after 96 h. In contrast, almost all cells in the control samples were alive in a 0.01 M NaCl solution for 72 h, but their numbers had started to decrease (<10%) by 96 h.

The FESEM photograph of the U(VI) accumulated yeast cells cultured on the YPD agar medium for 12 h (Fig. 10) showed that some yeast cells had not started budding (arrow heads in Fig. 10) and may have been in a resting mode or dead. The EDS analyses detected U and P on these cells.

4. DISCUSSION

4.1. Characteristics of U(VI)-Bearing Precipitates

Visible diffuse reflectance spectrometry showed that the U(VI)-bearing precipitates on the cells of yeast P1.0 at pHs 3.2 and 4.7 at 96 h were uranyl phosphate crystalline minerals. The SAED pattern (Fig. 7) had *d*-spacings of 4.9 and 3.5Å corresponding to the *d*-spacings of 110 and 020 of H-autunite, respectively (Burns, 1999). SEM-EDS and TEM-EDS spectra of these precipitates on yeast P1.0 at pH 3.2 at 96 h showed peaks of U and P (Fig. 5, spectra 4 and Fig. 8). Thus, H-autunite was precipitated on the yeast cells.

Minerals in the autunite and meta-autunite groups are easily dehydrated by evacuation. Butt and Graham (1981) reported

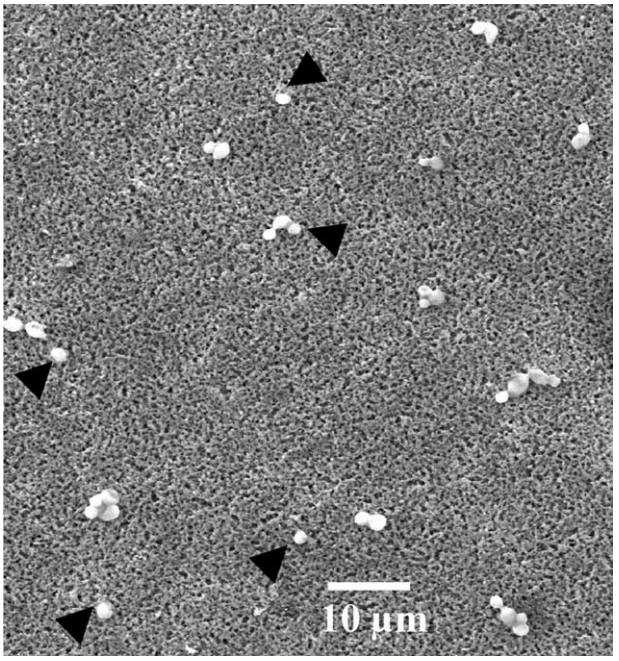

Fig. 10. FESEM image of U(VI) accumulated yeast grown on YPD agar medium for 12 h at 30°C. Arrows heads show nonbudding cells.

that dehydrated phases are structurally distinct from phases previously identified by X-ray diffraction (XRD). Since dehydration of H-autunite by evacuation changes their basal spacing (Suzuki et al., 2005), we showed reflections only from the a-b plane of H-autunite in the present study.

4.2. Accumulation Mechanisms of U(VI) by Yeast *S. cerevisiae*

Accumulation studies of U(VI) by microorganisms showed that U(VI) sorption is rapid and attains equilibrium within several h by surface complexation with cell-surface functional groups (Panak et al., 2000; Haas et al., 2001; Kelly et al., 2002; Francis et al., 2004). However, the time-dependent accumulation of U(VI) by yeast P1.0 appeared to be a two-step process (Fig. 1). The first step is fast, within several h. The second step proceeds more slowly, and equilibrium is not attained within 96 h. Up to 24 h after the exposure of yeast P1.0 at pHs 3.2 and 4.7 to U(VI) solution, the FESEM observation, the EDS spectra, and the visible absorbance spectra indicate that no U(VI) precipitate was formed, that the ratio of U M_α peak intensity to P K_α peak intensity was ~0.5, and that there was no detectable absorption peak of U(VI) phosphate minerals. Identical results were obtained for yeast P0.2. The amount of stored P in the cells of P0.2 probably is lower than that in yeast P1.0 because of the lower P content in the nutrient medium. Both yeasts accumulated the same fraction of U(VI) at pH 3.2, implying that the first step of U(VI) uptake by yeast is independent of the concentration of stored P.

Uranium(VI) adsorption by *Shewanella putrefaciens* is accounted for by the formation of surface complexes of >COO-UO_2^+ and >PO_4H-$UO_2(OH)_2$ (> represents the surface of bacteria; Haas et al., 2001). Characterization of the U(VI) adsorbed by *Bacillus* sp. showed the formation of inner-sphere complexes with the phosphate groups of the biomass (Panak et al., 2000), whereas X-ray absorption fine structure analysis of the adsorbed U(VI) by *B. subtilis* revealed that the uranium was associated with carboxyl functional groups on the bacterial surface (Kelly et al., 2002). Chmielowski et al. (1994) suggested that phosphate groups of mannans, that is, condensation polymers of mannose, which is a major component of the cell surface of *S. cerevisiae* (Volesky and May-Philips, 1995) are involved in U(VI) complexation. These results suggest that the first step in the U(VI) accumulation is sorption onto functional groups on the cell surface of the yeast, a conclusion that is supported by the thermodynamic calculation showing that the log Q/K was negative.

At 48 and 96 h after the U(VI) exposure, the peak intensity of U M_α was 0.5-fold that of the P K_α peak when no U(VI) precipitate was observed on the cells of yeast P1.0 at pH 3.2; identical results were obtained for yeast P0.2. This finding indicates that U(VI) is adsorbed on the cell surface. However, H-autunite was identified by FESEM-EDS and TEM-SAED analyses on the cell surfaces of yeast P1.0 at pH 3.2, forming directly there (Fig. 3e,f and Fig. 7, respectively). Thermodynamic calculations confirmed that if P and U(VI) concentrations are higher at the yeast cells' surfaces than in the bulk solution, H-autunite can be precipitated by local saturation (Table 1).

Equation 1 indicates that higher U and/or P concentrations in solution better stabilize or precipitate H-autunite than do lower concentrations. Hence, higher U(VI) and/or P concentrations should occur at the places where H-autunite developed than in bulk solution. Precipitation at the mineral's surface is controlled by the dissolution rates of solutes from a mineral because of the high diffusion of the solutes (e.g., Murphy et al., 1989), suggesting that H-autunite is unlikely to form at the boundary of the yeast cells and the bulk solution that is undersaturated with respect to H-autunite. TEM images of the yeast cells exposed to U(VI) solution showed that H-autunite developed at the ruptured regions of the cell surface but not on intact cells. Some yeast cells contained U(VI) precipitates. The concentration of P is probably higher inside the ruptured cell surface than in bulk solution. Since U(VI) is accumulated on the cells' surfaces, the concentration of U(VI) around the ruptured region should be higher than that in bulk solution. These results strongly suggest that the sorbed U(VI) on the surface of the yeast cells reacts with P liberated at the ruptured region of the cell surfaces, and consequently, H-autunite is formed by local saturation.

Yeast stores phosphate in its vacuoles (Okorokov et al., 1980). The stored P was released from yeast P1.0 into the solution containing U(VI) or a 0.01 mol · L^{-1} NaCl (Fig. 2). Soares et al. (2002) reported that *S. cerevisiae* NCNY 1190 releases P when it is exposed to Cd, Cu, and Pb. This release is attributed to uranium or heavy-metal toxicity (Soares et al., 2002; Bencheikh-Latmani and Leckie, 2003). Heavy metals induce lesions of the cell membrane of *S. cerevisiae* (Joho et al., 1984; Ohsumi et al., 1988), which may cause the cell to rupture.

The concentration of P released to the U(VI) solution is lower than that liberated to 0.01 mol · L^{-1} NaCl solutions of pHs 3.2 and 4.7 (Fig. 2). The released P should be partially consumed by the formation of H-autunite. If 10% of the sorbed U is used in this way, then the calculated concentration of P released to the U(VI) solution would be 4×10^{-5} mol · L^{-1}, that is, 10 times higher than the measured one. This consumption results in a higher concentration of P being released into U(VI) solution than into a 0.01 M NaCl solution.

For yeast P1.0 at pH 4.7, thermodynamic calculations (Table 1) and FESEM analyses (Fig. 4d) showed that H-autunite can form directly on the cells by simple precipitation. These findings suggest that the sorbed U(VI) on the cells' surface reacts with the P released from the cells to precipitate H-autunite, as was found for yeast P1.0 at pH 3.2. Thus, H-autunite occurs on the cells by local saturation and merely by precipitation in the bulk solution at pH 4.7.

The morphology of H-autunite formed on the yeast cells at pH 3.2 and pH 4.7 after 96 h U(VI) exposure differs. The morphology of crystals is affected by many factors, such as growth rate, impurity, and ionic strength (e.g., Ayati and Madsen, 2000). Differences in the thermodynamic conditions of formation of H-autunite at these pHs may be one of the reasons. Further experiments are warranted to examine the immediate cause of the morphologic difference.

The formation of H-autunite around the cells of *Citrobacter* sp. was reported by Macaskie et al. (1992), Young and Macaskie (1995), and Jeong et al. (1997). Phosphorus liberated from glycerol 2-phosphate in the solution reacted with the sorbed U(VI) on the membrane phospholipids to generate H-

autunite. Unfortunately, these authors did not discuss the thermodynamic conditions under which H-autunite formed around *Citrobacter* sp. Volesky and May-Phillips (1995) observed needlelike fibrils, ~2-μm long, on cell surface of *S. cerevisiae* by TEM after exposure to a 4.2×10^{-4} mol · L^{-1} U(VI) solution at pH 4 for 2 h. In the present study, we saw no U(VI)-phosphate minerals absorbance peak in the visible reflection spectrum of the U(VI) accumulated yeast at 24 h after exposure. We demonstrated that H-autunite formation depends on P concentration in the preculture medium. However, Volesky and May-Philips (1995) did not consider either the concentration of P in the U(VI) solution or the thermodynamics involved. Uranium(VI) was precipitated inside the cells of *Pseudomonas fluorescens* where the cell surfaces appeared to have ruptured (Krueger et al., 1993), a finding similar to our results. Unfortunately, Krueger et al. did not analyze the U(VI) mineral phases nor the geochemical conditions of precipitation.

Murakami et al. (1997) reported that saléeite ($Mg(UO_2)_2(PO_4)_2 \cdot 10H_2O$) forms on apatite even when groundwater is undersaturated with it. Radiation damage analysis of the formed material suggests that some of it has been preserved more than 10^5 years. They believe that the long-term containment of U(VI) was achieved by the formation of U(VI)-phosphate mineralization, but not by sorption on minerals. These results suggest that H-autunite mineralization is more durable than adsorption on the yeast cell surfaces, even after the yeast cells are lysed. The mineralization of saléeite proceeds in the leached layer of the dissolving apatite by local saturation. Ohnuki et al. (2004) suggest that P and Ca dissolved from apatite reacts with the sorbed U at the leached layer. This U(VI) mineral formation resembles the process we assumed in the present study, although P is provided by an abiotic resource.

Phosphorous is an essential element for bacteria. Certain microorganisms, such as *Microlunatus phosphovorous,* that store P in their cells have been isolated in activated sludge (Nakamura et, 1995). The heterotrophic denitrifier, *Paracoccus denitrificans*, as well as the denitrifying *Pseudomonas* sp. and *P. aeruginosa* among the ubiquitous bacteria in the soil environments, showed atypically high polyphosphate accumulation (Barak and van Rijn, 2000; Lacoste et al., 1981).

5. CONCLUSIONS

Our investigations of U(VI) accumulation by the yeast *S. cerevisiae* show that H-autunite may form on the cells even though the solution in which they are immersed is undersaturated with respect to H-autunite. TEM analysis of thin sections of the U(VI) accumulated yeast cells showed that H-autunite directly developed at the ruptured region of the cell surfaces. In thermodynamic calculations, 10 times higher concentrations of U(VI) and P on the cells than in bulk solution reflected supersaturation conditions for H-autunite formation. These results strongly suggest that the sorbed U(VI) on the cells' surfaces reacts with P released from the yeast to form H-autunite, not only by mere precipitation, but also by local saturation at the ruptured region. Hence, the yeast's cell surfaces, rather than the bulk solution, offer the specific conditions for this geochemical process. Thus, U(VI)-phosphate mineralization by local saturation at ruptured regions of the cell walls of microorganisms is one of the important uptake mechanisms of U(VI) and should be taken into account in predicting U(VI) mobility in the environment.

Acknowledgments—The authors are indebted to Professor T. Murakami of the University of Tokyo for thermodynamic calculations, and to Dr. R. Yasuda, Japan Atomic Energy Research Institute for assistance with the FESEM-EDS analysis. We would like to thank two anonymous reviewers and Dr. J. R. Haas for their constructive comments. Part of the present study was supported by a Grant-in-Aid of the Ministry of Education, Culture, Sports, Science and Technology to T.O.

Associate editor: J. R. Haas

REFERENCES

Ayati M. and Madsen H. E. L. (2000) Crystallization of some heavy-metal phosphates alone and in the presence of calcium ion. *J. Cryst. Growth* **208,** 579–591.

Barak Y. and van Rijn J. (2000) Atypical polyphosphate accumulation by the denitrifying bacterium *Paracoccus denitrificans. Appl. Environ. Microbiol.* **66,** 1209–1212.

Bencheikh-Latmani R. and Leckie J. O., (2003) Association of uranyl with the cell wall of *Pseudomonas fluorescens* inhibits metabolism. *Geochim. Cosmochim. Acta* **67,** 4057–4066.

Bennet D. G. and Read D. (1992) *Alligator Rivers Analogue Project Final Report* 10, DOE/HMIP/RP/92/080, Australian Nuclear Science and Technology Organisation.

Bruno J., De Pablo J., Duro L., and Figuerola E. (1995) Experimental study and modeling of the U(VI)-$Fe(OH)_3$ surface precipitation/coprecipitation equilibria. *Geochim. Cosmochim. Acta* **59,** 4113–4123.

Burns P. C. (1999) The crystal chemistry of uranium. In *Uranium: Mineralogy, Geochemistry and the Environment,* Reviews in Mineralogy Vol. 38 (ed. P.C. Burns and R. Finch), pp. 23–90, Mineralogical Society of America.

Butt C. R. M. and Graham J. (1981) Sodian potassian hydrooxonian? OK meta-autunite: first natural occurrence of an intermediate member of a predicted solid series. *Am. Mineral.* **66,** 1068–1072.

Chmielowski J., Worznica A., and Klapcinska B. (1994) Binding of uranium by yeast cell wall polysaccharides. *Bull. Polish Acad. Sci. Biol.* **42,** 147–149.

Duff M. C., Coughlin J. U., and Hunter D. B. (2002) Uranium coprecipitation with iron oxide minerals. *Geochim. Cosmochim. Acta* **66,** 3533–3547.

Francis A. J., Dodge C. J., Lu F., Halada G., and Clayton C. R. (1994) XPS and XANES studies of uranium reduction by *Clostridium* sp. *Environ. Sci. Technol.* **28,** 636–639.

Francis A. J., Gillow J. B., Dodge C. J., Harris R., Beveridge T. J., and Papenguth H. W. (2004) Uranium association with halophilic and nonhalophilic bacteria and archaea. *Radiochim. Acta* **92,** 481–488.

Grenthe I., Fuger J., Konings R. J. M., Lemire R. J., Muller A. B., Nguyen-Trung C., and Wanner H. (1992) *Chemical Thermodynamics, Volume 1: Chemical Thermodynamics of Uranium.* North-Holland.

Haas J. H., Dichristina T. J., and Wade R.Jr. (2001) Thermodynamics of U(VI) sorption onto *Shewanella putrifaciens*. *Chem. Geol.* **180,** 33–54.

Jeong B. C., Hawes C., Bonthrone K. M., and Macaskie L. E. (1997) Localization of enzymatically enhanced heavy metal accumulation *Citrobacter* sp. and metal accumulation in vitro by liposomes containing entrapped enzyme *Microbiology* **43,** 2497–2507.

Joho M., Ishibe A., and Murayama T. (1984) The injurious effect of heavy metal ions on the cell membrane in *Saccharomyces cerevisiae*. *Trans. Mycol. Soc. Japan* **25,** 485–488.

Kelly S. D., Kemner K. M., Fein J. B., Fowle D. A., Boyanov M. I., Bunker B. A., and Yee N. (2002) X-ray absorption fine structure determination of pH dependent U-bacterial cell wall interaction. *Geochim. Cosmochim. Acta* **66,** 3855–3871.

Knopp R., Panak P. J., Wray L. A., Renninger N. S., Keasling J. D., and Nitsche H. (2003) Laser spectroscopic studies of interactions of U^{VI} with bacterial phosphate species. *Chemistry Eur. J.* **9,** 2812–2818.

Krueger S., Olson G. L., Johnsonbaugh D., and Beveridge T. (1993) Characterization of the binding of gallium, platinum and uranium to Pseudomonas fluorescens by small-angle X-ray scattering and transmission electron microscopy. *Appl. Environ. Microbiol.* **59,** 4056–4064.

Kubelka P. and Munk F. (1931) Ein beitrag zur optik der farbanstriche. *Z. Tech. Phys.* **12,** 593–601.

Lacoste A. M., Cassaigne A., and Neuzil E. (1981) Transport of inorganic phosphate in *Pseudomonas aeruginosa*. *Curr. Microbiol.* **6,** 115–120.

Langmuir D. (1978) Uranium solution-minerals equilibria at low temperatures with applications to sedimentary ore deposits. *Geochim. Cosmochim. Acta* **42,** 547–569.

Lovley D. R., Phillips E. J. P., Gorby Y. A., and Landa E. R. (1991) Microbial reduction of uranium. *Nature* **350,** 413–416.

Lovley D. R., Widman P. K., Woodward J. C., and Phillips E. J. P. (1993) Reduction of uranium by cytochrome c3 of *Desulfovibrio desulfurican*. *Appl. Environ. Microbiol.* **59,** 3572–3576.

Macaskie L. E. and Dean A. C. R. (1985) Uranium accumulation by immobilized cells of *Citrobacter* sp. *Biotechnol. Lett.* **7,** 457–462.

Macaskie L. E., Empson R. M., Cheetham A. K., Grey C. P. A., and Skarnuli J. (1992) Uranium bioaccumulation by a *Citrobacter* sp. as a result of enzymatically mediated growth of polycrystalline HUO_2PO_4 *Science* **257,** 782–784.

Murakami T., Ohnuki T., Isobe H., and Sato T. (1997) Mobility of uranium during weathering. *Am. Mineral.* **82,** 888–899.

Murphy W. M., Oelkers E. H., and Lichtner P. C. (1989) Surface reaction versus diffusion control of mineral dissolution and growth rate in geochemical processes. *Chem. Geol.* **78,** 357–380.

Nagano T., Isobe H., Nakashima S., and Ashizaki M. (2002) Characterization of iron hydroxides in a weathered rock surface by visible microspectroscopy. *Appl. Spectrosc.* **56,** 651–657.

Nakamura K., Hiraishi A., Yoshimi Y., Kawaharasaki M., Masuda K., and Kamagata Y. (1995) *Microlunatus phosphovorous* gen. nov., sp. nov., A new Gram-positive polyphosphate accumulating bacteria isolated from activated sludge *Int. J. Syst. Bacteriol.* **45,** 17–22.

Ohnuki T., Kozai N., Samadfam M., Yasuda R., Yamamoto S., Narumi K., Naramoto H., and Murakami T. (2004) The formation of autunite $(CaUO_2)_2((PO_4)_2.nH_2O)$ within the leached layer of dissolving apatite: Uptake mechanisms of uranium by apatite. *Chem. Geol.* **211,** 1–14.

Ohsumi Y., Kitamoto K., and Anraku Y. (1988) Changes induced in the permeability barrier of the yeast plasma membrane by cupric ion. *J. Bacteriol.* **170,** 2676–2682.

Okorokov L. A., Kulakovslaya T. V., Lichko L. P., and Polorotova E. V. (1980) Vacuoles: main components of potassium, magnesium and phosphate ions in *Saccharomyces carlsbergensis* cells. *J. Bacteriol.* **144,** 661–665.

Panak P. J., Raff J., Selenska-Pobell S., Geipel G., Bernhard G., and Nitsche H. (2000) Complex formation of U(VI) with bacillus-isolates from a uranium mining waste pile. *Radiochim. Acta* **88,** 71–76.

Soares E. V., Duarte A. P. R. S., Boaventura R. A., and Soares H. M. V. M. (2002) Viability and release of complexing compounds during accumulation of heavy metals by a brewer's yeast. *Appl. Microbiol. Biotechnol.* **58,** 836–841.

Strandberg G. W., Shumate S. E., and Parrott J. R. (1981) Microbial cells as biosorbents for heavy metals: Accumulation of uranium by *Saccharomyces cerevisiae* and *Pseudomonas aeruginosa. Appl. Environ. Microbiol.* **41,** 237–245.

Suzuki Y. and Banfield J. F (1999) Geomicrobiology of uranium. In *Uranium: Mineralogy, Geochemistry and the Environment,* Reviews in Mineralogy Vol. 38 (ed. P.C. Burns and R. Finch), pp. 393–432, Mineralogical Society of America.

Suzuki Y., Sato T., Isobe H., Kogure T., and Murakami T. (2005) Dehydration processes of the meta-autunite group minerals, meta-autunite, metasaléeite and metatorbernite. *Am. Mineral.* **90,** 1308–1314.

Volesky B. and May-Philips H. A. (1995) Biosorption of heavy metals. *Biotechnol. Prog.* **11,** 235–250.

Young P. and Macaskie L. E. (1995) Role of citrate as complexing ligand which permits enzymatically-mediated uranyl ion bioaccumulation. *Bull. Environ. Contam. Toxicol.* **54,** 892–899.

Wolery T. J. (1992) *EQ3NR, A Computer Program for Geochemical Aqueous Speciation-Solubility Calculation: Theoretical Manual, User's Guide and Related Documentation,* Version 7.0, UCRL-MA-110662 PT III, Lawrence Livermore Laboratory, University of California.